

Conformational statistics of bent semiflexible polymers

Yu Zhou and Gregory S. Chirikjian^{a)}

Department of Mechanical Engineering, Johns Hopkins University, Baltimore, Maryland 21218

(Received 31 December 2002; accepted 9 June 2003)

This paper extends previous methods for obtaining the probability distribution function of end-to-end distance for semiflexible polymers, and presents a general formalism that can generate conformational statistics of any continuum filament model of semiflexible chains with internal bends and twists. In particular, our focus is distribution functions for chains composed of straight or helical segments connected with discrete bends or twists. Prior polymer theories are not able to fully account for the effects of these internal shape discontinuities. We use the operational properties of the noncommutative Fourier transform for the group of rigid-body motions in three-dimensional space. This general method applies to various stiffness models of semiflexible chainlike macromolecules. Examples are given which apply the stiffness parameters defined in the Kratky–Porod model, Yamakawa helical wormlike chain model, and revised Marko–Siggia double-helix model to chains with intrinsic bends or twists in their undeformed (minimal energy) state. We demonstrate how the location and magnitude of internal bends in the chain affect the distribution of end-to-end distances for each of these models. This capability allows one to study the entropic effects of intrinsic shape changes (e.g., bend angle) in various models, and may lead to coarse-grained continuum mechanical models of processes that occur during transcription regulation. © 2003 American Institute of Physics. [DOI: 10.1063/1.1596911]

I. INTRODUCTION

The statistical mechanics of DNA and other semiflexible (wormlike) chains has received much attention in the literature. Many models have been put forth to predict the behavior of semiflexible chains and to explain experimental data. Among those models, the freely jointed chain¹ and Kratky–Porod (wormlike chain) model^{2–4} are widely used to describe intrinsically straight polymer molecules. As an important extension, Yamakawa introduced the more general helical wormlike chain model.⁵ The mechanical stiffness of double-helical DNA has interested researchers since the late 1970s.⁶ During the last ten years, experimental measurements of these properties has received considerable attention.^{7–9} The Marko–Siggia¹⁰ and revised Marko–Siggia¹¹ double-helix chain models have been introduced recently to describe the coupling of DNA stiffness parameters.

A large body of work on polymer theory has sought to estimate the probability distribution and mean values of conformational properties such as end-to-end distance and radius of gyration. Common techniques are Monte Carlo, matrix-generator, and direct enumeration.^{12–20} Path integration can also be applied to provide “compact” analytical expressions. For some basic polymer models, “closed-form” path integral formulas have been derived for the probability distributions of loop length,²¹ segmental orientations,²² trajectories of a segment,²³ radius of gyration,²⁴ end-to-end position and distance,^{25–32} and moments.^{29,32,33} However, for sophisticated models, the evaluation of path integrals can be hard to handle, and usually requires extensive numerical calcula-

tions. In previous work we showed that the probability density function (PDF) of the end-to-end relative position and orientation for the most general model of an inextensible semiflexible polymer chain can be obtained by either solving a diffusion equation or convolving PDFs for short segments of the chain.^{34–37} In doing so, the exponential growth in the size of the sample space encountered in Monte Carlo and numerical path-integral methods is circumvented. More importantly, our model can generate the full six-degree-of-freedom probability distribution of relative position and orientation. This contains much more information than the probability distribution of end-to-end distance and its moments. The distribution of end-to-end distance is only a one-dimensional marginal PDF of the six-dimensional distribution that our method is capable of computing.

Whereas all of the studies mentioned above assume intrinsically straight or helical polymer chains, this paper presents a general formalism that can generate conformational statistics of any continuum filament model of semiflexible chains with internal bends and twists. The focus of this paper is to compute probability distributions for these bent and twisted semiflexible chains. First discovered in the early 1980s,³⁸ intrinsically bent DNAs are receiving more and more attention (for example, see Fig. 1). Bent DNAs have been observed and studied experimentally.^{39–46} In addition, models have been proposed to describe the relationship between bending stiffness and DNA sequence.^{47–49} However, classical semiflexible polymer theories such as the KP model are inadequate to describe the conformational statistics of these systems. Matrix-generator and Monte Carlo methods were used to study the influence of thermal fluctuation on the size and shape of bent DNA.⁵⁰ Work was done by Rivetti *et al.* to extend the applicability of the KP wormlike chain

^{a)}Author to whom correspondence should be addressed. Electronic mail: gregc@jhu.edu; Phone: 410-516-7127; Fax: 410-516-7254.

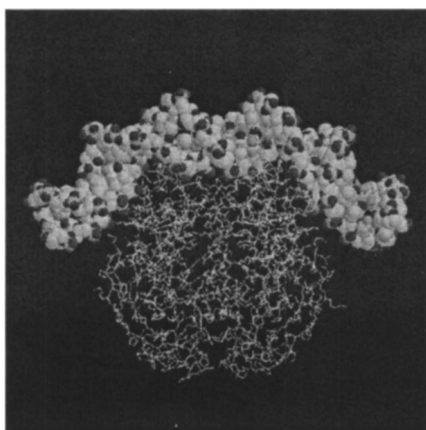


FIG. 1. CAP (1run.pdb): the DNA is a bent semiflexible polymer.

model to polymers containing bends.⁵¹ As a result, closed-form expressions for mean square end-to-end distance were derived. However, no previous work has been published on how to calculate the full probability distributions of bent macromolecules with arbitrary chirality and stiffness parameters. As an example of the importance of being able to compute statistical properties of intrinsically bent semiflexible chains (and hence the associated entropic forces), we are motivated by CAP as depicted in Fig. 1.⁴⁶

Most research on semiflexible polymer statistics is based on wormlike chain models. It has been shown in recent work that one methodology can be used to unify all previous statistical models of short wormlike chains in dilute solution.³⁴ As an example of this generality, it was shown to include the Kratky-Porod, Yamakawa, Marko-Siggia, and revised Marko-Siggia models as subcases. That general model, with the stiffness and chirality left as input parameters, is the starting point for this paper. In that model, the probability density function of the end-to-end relative pose (position and orientation) of a semiflexible polymer chain with nonbent minimal energy conformation can be obtained by solving a partial differential equation which was derived from a path integral formalism. Pose statistics are directly relevant to the case when internal bends and twists are present in a semiflexible chain, because such relationships are rigid-body motions that can generally not be described with the simple classical models. On the basis of the above-mentioned general statistical model, this paper proposes a method for computing the probability density function of end-to-end relative pose for intrinsically bent semiflexible chainlike macromolecules. Ignoring interactions between distal segments of the same polymer chain (which is reasonable for stiff chains that are short enough to make self contacts unlikely), our method applies to semiflexible inextensible chiral elastic macromolecules with internal bends and twists.

II. A GENERAL NONBENT SEMIFLEXIBLE POLYMER MODEL

Let \mathbf{R} be a rotation matrix parameterized by ZXZ Euler angles, and let \mathbf{a} be a position vector in 3D space parameterized by spherical coordinates. That is,

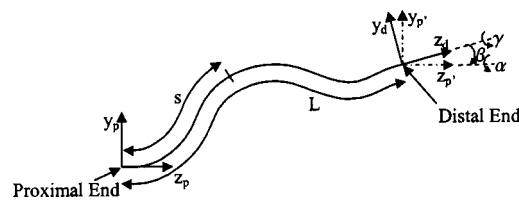


FIG. 2. Relationship between reference frames fixed at proximal and distal ends. (x_p, y_p, z_p) represents the frame of reference at the proximal end, (x_p', y_p', z_p') represents a frame located at the distal end but parallel to the frame of reference at the proximal end, and (x_d, y_d, z_d) represents the frame of reference at the distal end.

$$\mathbf{a} = \begin{pmatrix} a_1 \\ a_2 \\ a_3 \end{pmatrix} = \begin{pmatrix} a \sin \theta \cos \phi \\ a \sin \theta \sin \phi \\ a \cos \theta \end{pmatrix}, \quad (1)$$

where θ and ϕ are, respectively, the polar and azimuthal angles of \mathbf{a} , and

$$\mathbf{R} = \mathbf{R}(\alpha, \beta, \gamma) = \text{ROT}[\mathbf{e}_3, \alpha] \text{ROT}[\mathbf{e}_1, \beta] \text{ROT}[\mathbf{e}_3, \gamma], \quad (2)$$

where $\text{ROT}[\mathbf{e}_i, \varphi]$ denotes the rotation matrix describing counterclockwise rotation by φ about the natural basis vector \mathbf{e}_i which has elements $(\mathbf{e}_i)_j = \delta_{i,j}$. Here $\delta_{i,j}$ is the Kronecker delta function. The pair (\mathbf{a}, \mathbf{R}) describes the pose (position and orientation) of a frame of reference in space, or equivalently, the rigid-body motion required to move to the pose (\mathbf{a}, \mathbf{R}) from a reference frame defined by the identity orientation and zero translation, $(\mathbf{0}, \mathbf{1})$. In this paper, this pair (\mathbf{a}, \mathbf{R}) represents the relative pose between two frames of reference: one attached at the proximal end of a semiflexible polymer, and the other attached at the distal end. Each pair (\mathbf{a}, \mathbf{R}) can be thought of as an element of the group of rigid-body motions in three-dimensional space. This six-dimensional non-commutative Lie group is called SE(3)—the Special Euclidean group of three-dimensional space.³⁵ The group law is the composition of rigid-body motions.

We define a local frame of reference attached to the polymer backbone such that the \mathbf{e}_3 direction of this frame points along the tangent of the backbone of the polymer (see Fig. 2).

When a polymer is modeled as an inextensible chiral elastic chain, the position of any point at arc length s with respect to the frame of reference at the proximal end is

$$\mathbf{a}(s) = \int_0^s \mathbf{R}(\epsilon) \mathbf{e}_3 d\epsilon. \quad (3)$$

The elastic energy in the polymer is

$$E = \int_0^L U ds, \quad (4)$$

where L is the total length of the polymer and

$$U = \frac{1}{2} \boldsymbol{\omega}(s)^T \mathbf{B} \boldsymbol{\omega}(s) - \mathbf{b}^T \boldsymbol{\omega}(s) + c. \quad (5)$$

Here \mathbf{B} is a positive semidefinite symmetric matrix called the stiffness matrix, \mathbf{b} is a vector describing the chirality, c is a constant, and $\boldsymbol{\omega}(s)$ is the spatial angular velocity of the polymer (when s is interpreted as time rather than arc length) which satisfies

$$\boldsymbol{\omega}(s) \times \mathbf{r} = \mathbf{R}^T \frac{d\mathbf{R}}{ds} \mathbf{r}, \quad \forall \mathbf{r} \in R^3. \quad (6)$$

When $\boldsymbol{\omega}(s) = \mathbf{B}^{-1} \mathbf{b}$, U is minimized. This constant angular velocity yields a helical conformation of the polymer. Denoting $\omega = |\boldsymbol{\omega}|$, and $[n_1, n_2, n_3]^T = \boldsymbol{\omega}/\omega$, one can obtain the following closed-form formula for $\mathbf{a}(s)$ for an inextensible chiral elastic chain in this lowest energy conformation,

$$\mathbf{a}(s) = \begin{pmatrix} \frac{n_2}{\omega} (1 - \cos \omega s) + n_1 n_3 \left(s - \frac{1}{\omega} \sin \omega s \right) \\ \frac{n_1}{\omega} (\cos \omega s - 1) + n_2 n_3 \left(s - \frac{1}{\omega} \sin \omega s \right) \\ s - (n_1^2 + n_2^2) \left(s - \frac{1}{\omega} \sin \omega s \right) \end{pmatrix}. \quad (7)$$

When the chiral (helical) polymer is deformed from this shape, U increases.

Defining $\mathbf{D} = [D_{lk}] = \mathbf{B}^{-1}$ and $\mathbf{d} = [d_l] = -\mathbf{B}^{-1} \mathbf{b}$, one can obtain the following diffusion equation that describes how the PDF of relative pose between the frame of reference at arc length s and that at the proximal end of the chain evolves:^{34,35}

$$\frac{\partial f(\mathbf{a}, \mathbf{R}, s)}{\partial s} = \left(\frac{1}{2} \sum_{k,l=1}^3 D_{lk} \tilde{X}_l^R \tilde{X}_k^R + \sum_{l=1}^3 d_l \tilde{X}_l^R - \tilde{X}_6^R \right) f(\mathbf{a}, \mathbf{R}, s), \quad (8)$$

with initial conditions $f(\mathbf{a}, \mathbf{R}, 0) = \delta(\mathbf{a}) \delta(\mathbf{R})$, where δ is the Dirac delta function. Here \tilde{X}_i^R are differential operators for the group of rigid-body motions, SE(3), where $1 \leq i \leq 6$. These are analogous to directional derivatives for functions of Cartesian position. Using ZXZ Euler angles α , β , and γ to parameterize rotation \mathbf{R} , these operators have the following explicit form:

$$\begin{aligned} \tilde{X}_1^R &= \csc \beta \sin \gamma \frac{\partial}{\partial \alpha} + \cos \gamma \frac{\partial}{\partial \beta} - \cot \beta \sin \gamma \frac{\partial}{\partial \gamma}, \\ \tilde{X}_2^R &= \csc \beta \cos \gamma \frac{\partial}{\partial \alpha} - \sin \gamma \frac{\partial}{\partial \beta} - \cot \beta \cos \gamma \frac{\partial}{\partial \gamma}, \\ \tilde{X}_3^R &= \frac{\partial}{\partial \gamma}, \\ \tilde{X}_4^R &= (\cos \gamma \cos \alpha - \sin \gamma \sin \alpha \cos \beta) \frac{\partial}{\partial a_1} \\ &\quad + (\cos \gamma \sin \alpha - \sin \gamma \cos \alpha \cos \beta) \frac{\partial}{\partial a_2} \\ &\quad + \sin \beta \sin \gamma \frac{\partial}{\partial a_3}, \end{aligned} \quad (9)$$

$$\begin{aligned} \tilde{X}_5^R &= (-\sin \gamma \cos \alpha - \cos \gamma \sin \alpha \cos \beta) \frac{\partial}{\partial a_1} \\ &\quad + (-\sin \gamma \sin \alpha - \cos \gamma \cos \alpha \cos \beta) \frac{\partial}{\partial a_2} \\ &\quad + \sin \beta \cos \gamma \frac{\partial}{\partial a_3}, \end{aligned}$$

$$\tilde{X}_6^R = \sin \beta \sin \alpha \frac{\partial}{\partial a_1} - \sin \beta \cos \alpha \frac{\partial}{\partial a_2} + \cos \beta \frac{\partial}{\partial a_3}.$$

In previous work,³⁴ a methodology for solving equations such as Eq. (8) was developed based on operational properties of the Fourier transform for SE(3). The matrix elements of this transform are^{35,52}

$$\hat{f}_{l',m';l,m}^r(p) = \int_{SE(3)} f(\mathbf{a}, \mathbf{R}) \overline{U_{l,m;l',m'}^r(\mathbf{a}, \mathbf{R}; p)} d\mathbf{R} d\mathbf{a}, \quad (10)$$

where $d\mathbf{R} d\mathbf{a} = (1/8\pi^2) \sin \beta d\alpha d\beta d\gamma \sin \theta a^2 da d\theta d\phi$ is the invariant integration measure for SE(3). The desired PDF can be obtained by the inverse transform^{35,52}

$$\begin{aligned} f(\mathbf{a}, \mathbf{R}) &= \frac{1}{2\pi^2} \sum_{r=-\infty}^{\infty} \sum_{l'=|r|}^{\infty} \sum_{l=|r|}^{\infty} \sum_{m'=-l'}^{l'} \sum_{m=-l}^l \int_0^{\infty} \hat{f}_{l,m;l',m'}^r(p) \\ &\quad \times U_{l',m';l,m}^r(\mathbf{a}, \mathbf{R}; p) p^2 dp, \end{aligned} \quad (11)$$

where $U_{l',m';l,m}^r(\mathbf{a}, \mathbf{R}; p) = \sum_{j=-l}^l [l', m' | p, r | l, j] (\mathbf{a}) U_{j,m}^l(\mathbf{R})$ are the elements of the infinite-dimensional irreducible unitary representation matrices of the group SE(3).^{35,52-54} Here $U_{mn}^l(\mathbf{R})$ are matrix elements of the irreducible unitary representation of the group of rotations SO(3),^{35,55}

$$U_{mn}^l(\mathbf{R}(\alpha, \beta, \gamma)) = (-1)^{n-m} e^{-i(m\alpha+n\gamma)} P_{m,n}^l(\cos \beta), \quad (12)$$

where $P_{m,n}^l(x)$ are generalized Legendre functions,

$$\begin{aligned} P_{m,n}^l(\cos \beta) &= \left[\frac{(l-m)!(l+m)!}{(l-n)!(l+n)!} \right]^{1/2} \\ &\quad \times \sin^{m-n} \frac{\beta}{2} \cos^{m+n} \frac{\beta}{2} P_{l-m}^{(m-n, m+n)}(\cos \beta), \end{aligned} \quad (13)$$

and $P_l^{(m,n)}(x)$ are the Jacobi polynomials. Meanwhile,

$$\begin{aligned} [l', m' | p, r | l, m] (\mathbf{a}) &= \frac{1}{\sqrt{4\pi}} \sum_{k=|l'-l|}^{l'+l} i^k \sqrt{\frac{(2l'+1)(2k+1)}{(2l+1)}} j_k(pa) \\ &\quad \times C(k, 0; l', r | l, r) C(k, m-m'; l', m' | l, m) \\ &\quad \times Y_k^{m-m'}(\theta, \phi), \end{aligned} \quad (14)$$

where $j_k(x)$ is the k th spherical Bessel functions, $Y_k^m(\theta, \phi)$ are spherical harmonics, and $C(a, \alpha; b, \beta | c, \gamma)$ are Clebsch–Gordan coefficients.³⁵ By applying the Fourier transform for SE(3) on both sides of Eq. (8), one can obtain the following system of linear ordinary differential equations with constant coefficients:

$$\frac{d\hat{\mathbf{f}}^r}{ds} = \mathbf{B}^r \hat{\mathbf{f}}^r. \quad (15)$$

This is because of operational properties of the SE(3)-Fourier transform which convert \tilde{X}_i^R operators into linear algebraic operations in the SE(3) dual space.³⁵ The elements of \mathbf{B}^r have the explicit form,

$$\begin{aligned} B_{l',m';l,m}^r = & \Lambda_{m',m}^l \delta_{l',l} - i p \kappa_{l',m'}^r \delta_{l'-1,l} \delta_{m',m} \\ & - i p \frac{m' r}{l'(l'+1)} \delta_{l',l} \delta_{m',m} \\ & - i p \kappa_{l,m}^r \delta_{l',l-1} \delta_{m',m}. \end{aligned} \quad (16)$$

Here,

$$\kappa_{l',m'}^r = \left(\frac{(l'^2 - m'^2)(l'^2 - r^2)}{(2l'+1)(2l'-1)l'^2} \right)^{1/2}, \quad (17)$$

and all elements of Λ are zero except

$$\begin{aligned} \Lambda_{m,m+2}^l = & \left(\frac{D_{11} - D_{22}}{8} + \frac{i D_{12}}{4} \right) c_{m+1}^l c_{-m-1}^l, \\ \Lambda_{m,m+1}^l = & \left(\frac{(2m+1)(D_{23} - i D_{13})}{4} + \frac{d_1 + i d_2}{2} \right) c_{-m-1}^l, \\ \Lambda_{m,m}^l = & - \frac{D_{11} + D_{22}}{8} (c_{-m}^l c_{m-1}^l + c_m^l c_{-m-1}^l) \\ & - \frac{D_{33} m^2}{2} - i d_3 m, \end{aligned} \quad (18)$$

$$\begin{aligned} \Lambda_{m,m+1}^l = & \left(\frac{(2m+1)(D_{23} + i D_{13})}{4} + \frac{-d_1 + i d_2}{2} \right) c_{m-1}^l, \\ \Lambda_{m,m+2}^l = & \left(\frac{D_{11} - D_{22}}{8} - \frac{i D_{12}}{4} \right) c_{-m+1}^l c_{m-1}^l, \end{aligned}$$

where

$$c_n^l = \begin{cases} \sqrt{(l-n)(l+n+1)}, & l \geq |n| \\ 0, & \text{otherwise.} \end{cases} \quad (19)$$

Then, by solving Eq. (15), one obtains

$$\hat{\mathbf{f}}^r(p,s) = e^{s\mathbf{B}^r}. \quad (20)$$

Substituting the elements of $\hat{\mathbf{f}}^r$ into Eq. (11), one obtains the distribution of pose of the frame attached to the polymer at arc length s relative to the frame at $s=0$. When it is obvious which value of s is of interest we use the notation $\hat{\mathbf{f}}^r(p)$ in place of $\hat{\mathbf{f}}^r(p,s)$.

In practice, only an approximation to Eq. (20) is computed because the infinite-dimensional matrix \mathbf{B}^r is truncated before exponentiating. This step can be justified mathematically.⁵⁶

III. A GENERAL ALGORITHM FOR BENT AND TWISTED SEMIFLEXIBLE POLYMER CHAINS

A bent polymer chain is depicted in Fig. 3. As a frame traverses the backbone of the polymer chain, one can simply divide the chain into two segments. Each of these segments has a probability density function which describes the ensemble of all possible motions of the distal end of a chain segment relative to its own proximal end. Let the segments have arc length L_1 and L_2 , respectively. The interaction between the two segments is implemented by a full six-degree-of-freedom rigid-body motion. A bend or twist is a rotation at the separating point between the two segments with no trans-

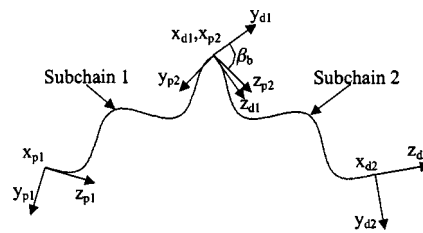


FIG. 3. Schematic diagram of a bent polymer chain. (x_p, y_p, z_p) represents the frame of reference at the proximal end, (x_d, y_d, z_d) represents the frame of reference at the distal end, and β_b represents the angle between the tangents to the backbone at the bend.

lation. As a result, the PDF of end-to-end pose for an intrinsically bent semiflexible chain is a convolution of three PDFs, each of which is a function of six pose variables (three position variables and three orientation variables),

$$f(\mathbf{a}, \mathbf{R}) = (f_1 * f_2 * f_3)(\mathbf{a}, \mathbf{R}). \quad (21)$$

Here $f_1(\mathbf{a}, \mathbf{R})$ is the pose probability distribution of the frame of reference attached at the distal end of subchain 1 relative to its own proximal end; f_3 is the pose probability distribution of the distal end of subchain 2 relative to its own proximal end; f_2 is the pose probability distribution of the frame of reference at the proximal end of subchain 2 relative to the frame at the distal end of subchain 1, describing the junction between the two subchains. Here $f_1(\mathbf{a}, \mathbf{R})$ is obtained by setting $s=L_1$ in Eq. (20) and substituting the result into Eq. (11), and $f_3(\mathbf{a}, \mathbf{R})$ is obtained by setting $s=L_2$ and following the same procedure. In contrast, $f_2(\mathbf{a}, \mathbf{R}) = \delta(\mathbf{a}) \delta(\mathbf{R}_b^{-1} \mathbf{R})$, where \mathbf{R}_b is the rotation made at the bend, and the fact that the delta function for SE(3) is the product of those for R^3 and SO(3) has been used. Notice that the delta function in translation is centered at the origin because the two subchains meet at a point rather than being translated in space relative to each other; meanwhile, the delta in rotation is centered on the relative orientation between the connected segments. The convolution in Eq. (21) is a convolution on the group SE(3).³⁷

$$(f_i * f_j)(\mathbf{g}) = \int_{SE(3)} f_i(\mathbf{h}) f_j(\mathbf{h}^{-1} \circ \mathbf{g}) d(\mathbf{h}), \quad (22)$$

where $\mathbf{g} = (\mathbf{a}, \mathbf{R})$ and \mathbf{h} denote members of SE(3). This is not to be confused with convolution in the sense most familiar to scientists and engineers. In the definition of convolution given in Eq. (22), the little circle is the group multiplication law for rigid-body motions. Previous work has made the connection between this kind of convolution and polymer statistics,³⁷ as well as provided algorithms for the efficient computation of this kind of convolution.⁵⁷

In the context of bent semiflexible polymer chains, the Fourier transform for SE(3) provides a relatively easy way to compute Eq. (21). By applying the transform on both sides of Eq. (21), one obtains

$$\hat{\mathbf{f}}^r(p) = \hat{\mathbf{f}}_3^r(p) \hat{\mathbf{f}}_2^r(p) \hat{\mathbf{f}}_1^r(p). \quad (23)$$

It is a general property that the Fourier transform of a convolution of functions is the product of the Fourier transforms of those functions multiplied in reverse order. Since in this

context the Fourier transforms are matrix-valued functions, the order of multiplication matters. One can compute $\hat{\mathbf{f}}_1^r$ and $\hat{\mathbf{f}}_3^r$ by using Eq. (20), and obtain $\hat{\mathbf{f}}_2^r$ as

$$\begin{aligned}\hat{f}_{2l',m';l,m}^r(p) &= \int_{\text{SE}(3)} f(\mathbf{a}, \mathbf{R}) \overline{U_{l,m;l',m'}^r(\mathbf{a}, \mathbf{R}; p)} d\mathbf{R} d\mathbf{a} \\ &= \int_{\text{SE}(3)} \delta(\mathbf{a}) \delta(\mathbf{R}_b^{-1} \mathbf{R}) \overline{U_{l,m;l',m'}^r(\mathbf{a}, \mathbf{R}; p)} d\mathbf{R} d\mathbf{a} \\ &= \overline{U_{l,m;l',m'}^r(\mathbf{0}, \mathbf{R}_b; p)} \\ &= (-1)^{(l'-l)} (-1)^{(m'-m)} \delta_{l,l'} \tilde{U}_{-m',-m}^l(\mathbf{R}_b) \\ &= (-1)^{(l'-l)} \delta_{l,l'} e^{im' \alpha_b} P_{m,n}^l(\cos \beta_b) e^{im \gamma_b},\end{aligned}\quad (24)$$

where α_b , β_b , and γ_b are ZXZ Euler angles of \mathbf{R}_b . By substituting the elements of $\hat{\mathbf{f}}^r$ into Eq. (11), one can compute the PDF of end-to-end pose of bent polymer chains. If α_b and γ_b are both zero but β_b is not zero, we call this a bent chain. In contrast if β_b is zero but α_b or γ_b is not zero, we call this a twisted chain.

Because the distribution of end-to-end distance and angle between the tangents at both the proximal end and the distal end are quantities that can be measured from experiments directly, these low-dimensional PDFs are of interest. The end-to-end distance is $a = |\mathbf{a}(L)|$, and the angle between the tangents at both ends is the β Euler angle of $\mathbf{R}(L)$. By using Eqs. (23) and (20) and integrating Eq. (11), one can obtain $f(a)$ from $f(\mathbf{a}, \mathbf{R})$ as

$$\begin{aligned}f(a) &= \frac{a^2}{2\pi^2} \int_0^\pi \int_0^{2\pi} \int_{\text{SO}(3)} f(\mathbf{a}, \mathbf{R}) \sin \theta d\mathbf{R} d\phi d\theta \\ &= \frac{2a^2}{\pi} \int_0^\infty \hat{f}_{0,0;0,0}^0(p) \frac{\sin pa}{pa} p^2 dp.\end{aligned}\quad (25)$$

Moreover, one can obtain $f(a, \beta)$ as

$$\begin{aligned}f(a, \beta) &= \frac{a^2 \sin \beta}{8\pi^2} \int_0^\pi \int_0^{2\pi} \int_0^{2\pi} \int_0^{2\pi} f(\mathbf{a}, \mathbf{R}) \sin \theta d\mathbf{R} d\phi d\gamma d\theta \\ &= \frac{a^2 \sin \beta}{2\pi} \int_0^\infty \left(\sum_{r=-\infty}^{\infty} \sum_{l=|r|}^{\infty} \hat{f}_{l,0;l,0}^r(p) P_l(\cos \beta) \right) \\ &\quad \times j_0(pa) p^2 dp,\end{aligned}\quad (26)$$

where $P_l(x)$ are Legendre polynomials.

IV. NUMERICAL RESULTS

By definition $r \in \mathbb{Z}$ (the integers) and $0 \leq p < \infty$, and \mathbf{B}^r is infinite dimensional. To do numerical computations, one must truncate \mathbf{B}^r at finite values of r , l , and p . We truncate at $r=r_B$, $l=l_B$, and $p=p_B$ such that $-r_B \leq r \leq r_B$, $-l_B \leq l \leq l_B$, and $0 \leq p \leq p_B$. When $f(a)$ is of interest, we only need to consider $r=0$, as suggested by Eq. (25). As far as units are concerned, “ a ” is a distance and L is an arc length. They can be measured in any length units that one chooses. In our computation, all the stiffness and length parameters are normalized by persistence length. The general formulation re-

viewed in Sec. II applies to several stiffness models. Numerical computations are now implemented with these different models.

The Kratky–Porod and Yamakawa models are well known in polymer theory. For the Kratky–Porod wormlike chain model, the stiffness matrix, chirality vector and constant in Eq. (5) are defined as²

$$\mathbf{B} = \begin{pmatrix} \alpha_0 & 0 & 0 \\ 0 & \alpha_0 & 0 \\ 0 & 0 & 0 \end{pmatrix}, \quad \mathbf{b} = \begin{pmatrix} 0 \\ 0 \\ 0 \end{pmatrix}, \quad c = 0, \quad (27)$$

where α_0 is the stiffness parameter, which is related to temperature T , Boltzmann constant k_B , and persistence length l_p as

$$\alpha_0 = k_B T l_p. \quad (28)$$

In Fig. 4, we compute as examples $f(a)$ and $f(a, \beta)$ for a Kratky–Porod chain with $\alpha_0=0.1$, $L_1=L_2=0.5$, and $\mathbf{R}_b = \mathbf{R}(0, \pi/4, 0)$. To compute $f(a, \beta)$, we set $r_B=l_B=3$, $p_B=50$; to compute $f(a)$, we set $l_B=6$, $p_B=120$. In general, different values of the physical parameters will result in different probability distributions. Knowing this is useful for determining the properties of a polymer chain, such as stiffness, from experimentally measured PDFs.

By changing the bend angle β_b over the range $[0, \pi]$, one can see how it affects the resulting PDFs of end-to-end dis-

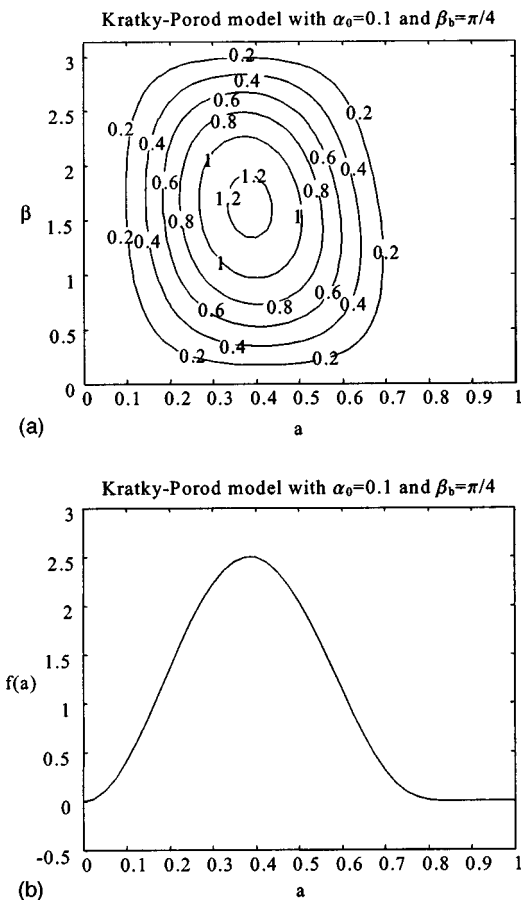


FIG. 4. $f(a, \beta)$ and $f(a)$ for the Kratky–Porod model with a bend. (a) Contour plot of $f(a, \beta)$. (b) Plot of $f(a)$.

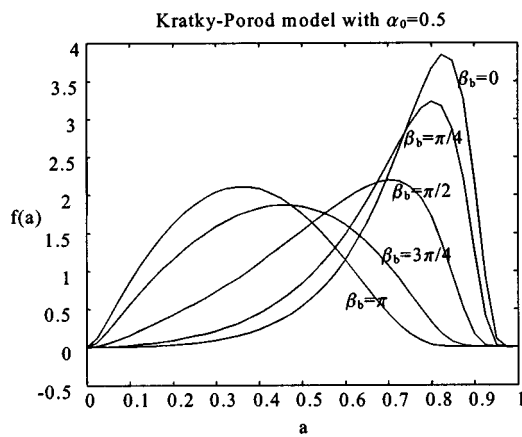


FIG. 5. Evolution of $f(a)$ with respect to bend angle for the Kratky–Porod model.

tance. By choosing $\alpha_0=0.5$, $L_1=L_2=0.5$, $l_B=6$, and $p_B=120$, we compute a set of $f(a)$ curves with different values of β_b for the Kratky–Porod model (Fig. 5).

By changing the bend location, L_1 , over the range of backbone arc length [0,0.5], one can see how it affects the resulting PDFs of end-to-end distance. By choosing $\alpha_0=0.5$, $\mathbf{R}_b=\mathbf{R}(0,\pi/2,0)$, $l_B=6$, and $p_B=120$, we computed a set of curves for $f(a)$ with different values of L_1 (where $L_1+L_2=1$) for the Kratky–Porod model (Fig. 6). Using these curves, one can identify the location of a bend from a PDF of end-to-end distance.

For the Yamakawa helical chain model, the stiffness matrix, chirality vector and constant in Eq. (3) are defined as⁵

$$\mathbf{B} = \begin{pmatrix} \alpha_0 & 0 & 0 \\ 0 & \alpha_0 & 0 \\ 0 & 0 & \beta_0 \end{pmatrix}, \quad \mathbf{b} = \begin{pmatrix} 0 \\ \alpha_0 \kappa_0 \\ \beta_0 \tau_0 \end{pmatrix},$$

$$c = \frac{1}{2}(\beta_0 \tau_0^2 + \alpha_0 \kappa_0^2), \quad (29)$$

where κ_0 and τ_0 are the curvature and torsion of the helix respectively, α_0 is defined as Eq. (28), and

$$\beta_0 = \alpha_0(1+\sigma)^{-1}, \quad (30)$$

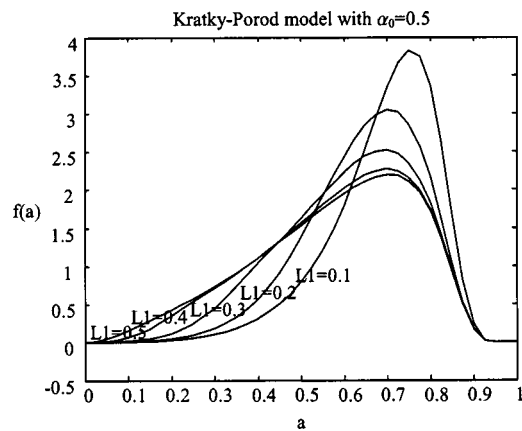


FIG. 6. Evolution of $f(a)$ with respect to position of bending point for Kratky–Porod model.

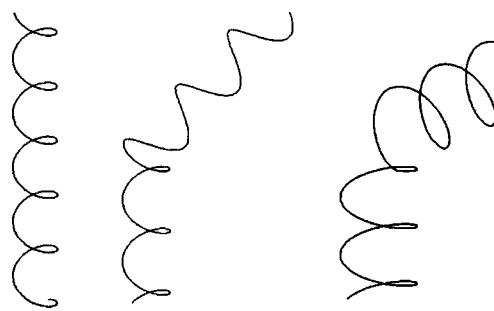


FIG. 7. Single-helical polymer chains modified from the Yamakawa model. The left is a nonbent helix, the middle is a bent helix, and the right is a twisted helix.

where σ is the Poisson ratio. With Eq. (7), one obtains helical chains as shown in Fig. 7.

In Fig. 8, we compute as examples $f(a)$ and $f(a,\beta)$ for a Yamakawa chain with $\alpha_0=0.1$, $\sigma=0$, $\kappa_0=\tau_0=30$, $L_1=L_2=0.5$, and $\mathbf{R}_b=\mathbf{R}(0,\pi/4,0)$. To compute $f(a,\beta)$, we set $r_B=l_B=3$, $p_B=50$; to compute $f(a)$, we set $l_B=6$, $p_B=120$.

To study the impact of bending angle, we chose $\alpha_0=0.5$, $\sigma=0$, $\kappa_0=\tau_0=30$, $L_1=L_2=0.5$, $l_B=6$, and $p_B=120$, and computed a set of curves for $f(a)$ with different values of the bending angle β_b for the Yamakawa model (Fig. 9).

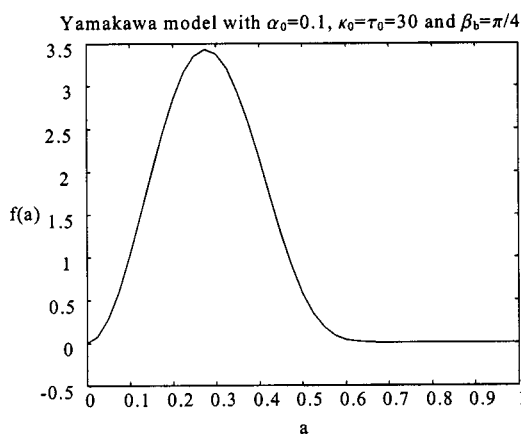
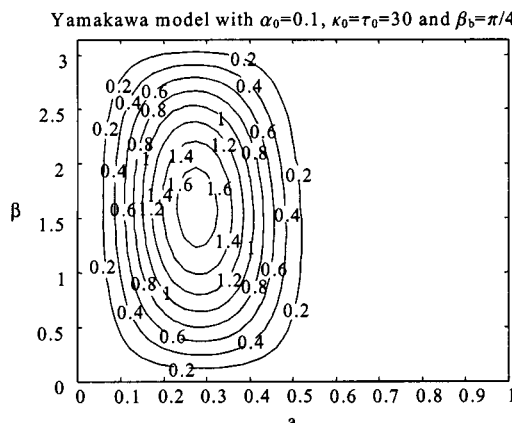


FIG. 8. $f(a,\beta)$ and $f(a)$ for the Yamakawa model. (a) Contour plot of $f(a,\beta)$. (b) Plot of $f(a)$.

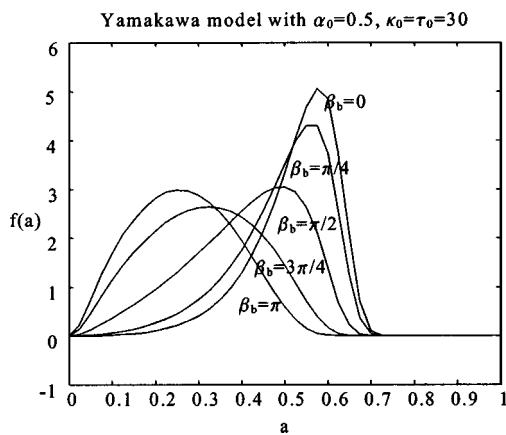


FIG. 9. Evolution of $f(a)$ with respect to bending angle for Yamakawa model with equal curvature and torsion.

By choosing $\alpha_0=0.5$, $l_B=6$, $p_B=120$, $L_1=L_2=0.5$, but $\kappa_0=5$, $\tau_0=1$, we obtain another set of curves for $f(a)$ with different values of β for the Yamakawa model, which shows quite different patterns caused by unequal curvature and torsion (Fig. 10).

For a polymer with a helical backbone such as a Yamakawa chain, a twist about the local e_3 direction will also affect the distribution of end-to-end relative pose. To study the impact of twisting angle, by choosing $\alpha_0=0.5$, $\sigma=0$, $\kappa_0=\tau_0=30$, $L_1=L_2=0.5$, $l_B=6$, and $p_B=120$, we compute a set of curves of $f(a)$ with different values of the twisting angle α_b for the Yamakawa model (Fig. 11) while keeping γ_b and β_b zero.

Because of its importance in studying double-stranded DNA molecules, we also use the revised Marko–Siggia model in which the stiffness matrix, chirality vector and constant in Eq. (3) are defined as¹¹

$$\mathbf{B} = \begin{pmatrix} \eta + \frac{\xi^2}{v} & 0 & \xi \\ 0 & \eta & 0 \\ \xi & 0 & v \end{pmatrix}, \quad \mathbf{b} = \begin{pmatrix} \xi \omega_0 \\ 0 \\ v \omega_0 \end{pmatrix}, \quad c = \frac{1}{2}v \omega_0^2, \quad (31)$$

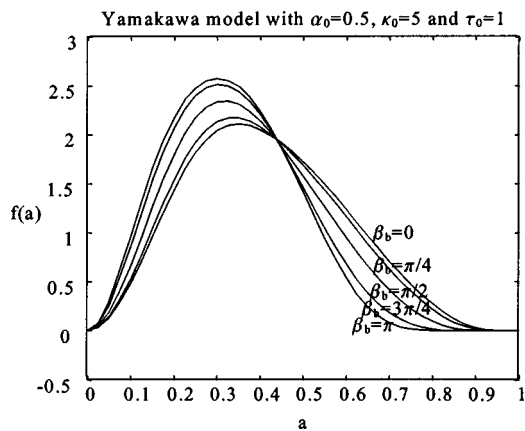


FIG. 10. Evolution of $f(a)$ with respect to bending angle for the Yamakawa model with different curvature and torsion.

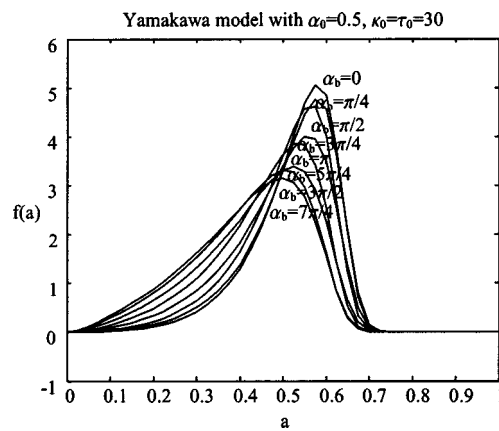


FIG. 11. Evolution of $f(a)$ with respect to twisting angle for the Yamakawa model.

where η is the bending persistent length, v is the twisting persistent length, ξ is the bend–twist coupling constant, and ω_0 is the spatial angular frequency of the helix. With Eq. (7), one obtains helical chains as shown in Fig. 12. Notice that the backbone of each segment is straight, only the double-helix twists about its axis.

In Fig. 13, we compute as examples $f(a)$ and $f(a, \beta)$ for the revised Marko–Siggia chain with $\eta=v=0.1$, $\xi=0.5$, $L_1=L_2=0.5$, $\omega_0=2\pi$, and $\mathbf{R}_b=\mathbf{R}(0, \pi/4, 0)$. To compute $f(a, \beta)$, we set $r_B=l_B=3$, $p_B=50$; to compute $f(a)$, we set $l_B=6$, $p_B=120$.

To study the impact of bending angle, by choosing $\eta=v=\xi=0.5$, $l_B=6$, $p_B=120$, $L_1=0.5$, $L_2=0.5$, $\omega_0=2\pi$, we compute a set of curves for $f(a)$ with different values of the bending angle β_b for the revised Marko–Siggia model (Fig. 14).

From Figs. 5, 9, 10, and 14, one observes the intuitive result that the peak of the polymer pose PDF will move towards the proximal end when the bending angle approaches π . The methodology presented here allows one to obtain for any model of semiflexible polymers with intrinsic shape discontinuities the probability density of relative end-to-end position and orientation (or any marginal probability density thereof, such as the end-to-end distance distribution). This capability allows one to study the entropic effects of shape changes (e.g., bend angle) in various models, and may

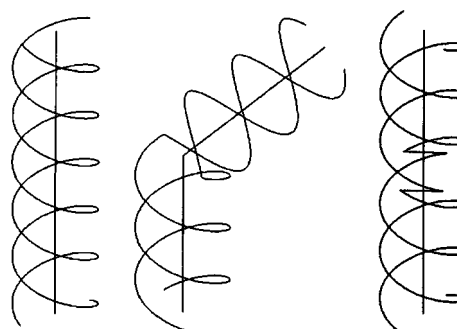


FIG. 12. Double-helical macromolecules corresponding to the revised Marko–Siggia model. The left is a nonbent double helix, the middle is a bent double helix, and the right is a twisted double helix.

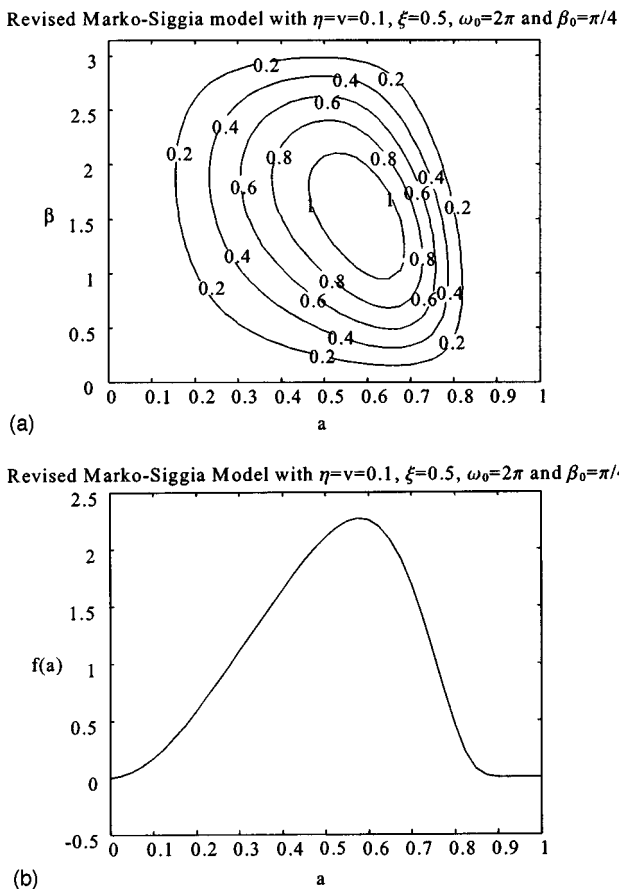


FIG. 13. $f(a, \beta)$ and $f(a)$ for the revised Marko–Siggia model. (a) Contour plot of $f(a, \beta)$. (b) Plot of $f(a)$.

lead to coarse-grained continuum mechanical models of processes that occur during transcription regulation.

V. CONCLUSION

This paper presents an efficient method for determining the conformational statistics of bent or twisted macromolecules given their stiffness, chirality and bend/twist parameters. Probability distributions on the six-dimensional group of rigid-body motions and the concept of motion-group con-

volution are applied to the connection of chain segments at the bend or twist. The representation theory and harmonic analysis for the Euclidean motion group are used to effectively compute the two convolutions involved in jointing two semiflexible chains at a bend or twist. Certain new and useful operational properties of the Fourier transform for the group of rigid-body motions are derived, which are directly relevant to the case of semiflexible polymers with bends and twists. With this general model, the 6D pose density for a semiflexible continuum filament with arbitrary chirality and anisotropic elasticity can be obtained. Examples are given to show how this general method applies to different models of macromolecules. This method can apply to chains with more than one bend by simply including more PDFs of nonbent segments and rotations concatenated by performing multiple convolutions. Moreover, it can apply to chains with not only bending but also twisting discontinuities. In fact, the proposed method applies to more general spatial relationships between two neighboring segments of a polymer chain, because any such relationship is a rigid-body motion.

ACKNOWLEDGMENTS

The authors thank Mr. Moonki Kim for generating the figure of CAP DNA (Fig. 1) from the PDB file 1run.pdb. This work was supported under NSF Grant No. IIS-0098382. The results and opinions expressed are only those of the authors.

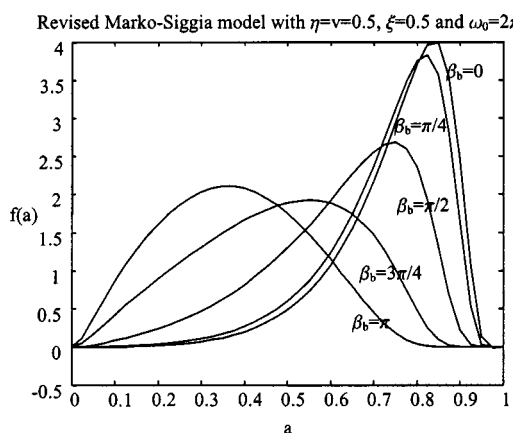


FIG. 14. Evolution of $f(a)$ with respect to bending angle for the revised Marko–Siggia model.

- ¹P. J. Flory, *Statistical Mechanics of Chain Molecules* (Interscience, New York, 1969).
- ²O. Kratky and G. Porod, *Recl. Trav. Chim. Pays-Bas* **68**, 1106 (1949).
- ³H. E. Daniels, *Proc. R. Soc. Edinburgh, Sect. A: Math. Phys. Sci.* **63**, 290 (1952).
- ⁴J. J. Hermans and R. Ullman, *Physica (Amsterdam)* **18**, 951 (1952).
- ⁵H. Yamakawa, *Helical Wormlike Chains in Polymer Solutions* (Springer, New York, 1997).
- ⁶A. V. Vologodskii, V. V. Anshelevich, A. V. Lukashin, and M. D. Frank-Kamenetskii, *Nature (London)* **280**, 294 (1979).
- ⁷J. D. Moroz and P. Nelson, *Proc. Natl. Acad. Sci. U.S.A.* **94**, 14418 (1997).
- ⁸J. D. Moroz and P. Nelson, *Macromolecules* **31**, 6333 (1998).
- ⁹T. B. Liverpool, R. Golestanian, and K. Kremer, *Phys. Rev. Lett.* **80**, 405 (1998).
- ¹⁰J. F. Marko and E. D. Siggia, *Macromolecules* **27**, 981 (1994).
- ¹¹H. Zhou and Z. Ou-Yang, *Phys. Rev. E* **58**, 4816 (1998).
- ¹²M. Fixman and R. Alben, *J. Chem. Phys.* **58**, 1553 (1973).
- ¹³R. C. Maroun and W. K. Olson, *Biopolymers* **27**, 561 (1988).
- ¹⁴P. J. Hagerman, *Biopolymers* **24**, 1881 (1985).
- ¹⁵M. Lax, A. J. Barrett, and C. Domb, *J. Phys. A* **11**, 361 (1978).
- ¹⁶C. A. Croxton, *J. Phys. A* **12**, 2475 (1979).
- ¹⁷K. H. Nitta, *J. Chem. Phys.* **101**, 4222 (1994).
- ¹⁸F. Aguilera-Granja and R. Kikuchi, *Physica A* **182**, 331 (1992).
- ¹⁹Q. Liao and D. C. Wu, *Acta Polym. SINCA* **4**, 420 (2000).
- ²⁰D. C. Wu, P. Du, and J. Kang, *Sci. China, Ser. B: Chem.* **40**, 137 (1997).
- ²¹T. B. Liverpool and S. F. Edwards, *J. Chem. Phys.* **103**, 6716 (1995).
- ²²J. Walasek, *J. Polym. Sci., Part B: Polym. Phys.* **26**, 1907 (1988).
- ²³S. F. Burlatskii and G. S. Oshanin, *Theor. Math. Phys.* **75**, 659 (1988).
- ²⁴S. R. Coriell and J. L. Jackson, *J. Math. Phys.* **8**, 1276 (1967).
- ²⁵M. K. Kosmas, *J. Phys. A* **16**, L381 (1983).
- ²⁶J. Wilhelm and E. Frey, *Phys. Rev. Lett.* **77**, 2581 (1996).
- ²⁷J. B. Lagowski, J. Noolandi, and B. Nickel, *J. Chem. Phys.* **95**, 1266 (1991).
- ²⁸G. Ronca and D. Y. Yoon, *J. Chem. Phys.* **80**, 930 (1984).
- ²⁹R. P. Mondescu and M. Muthukumar, *Phys. Rev. E* **57**, 4411 (1998).
- ³⁰R. P. Mondescu and M. Muthukumar, *J. Chem. Phys.* **110**, 12240 (1999).
- ³¹G. G. Hoffman, *J. Phys. Chem. B* **103**, 7167 (1999).

- ³²G. J. Papadopoulos and J. Thomchick, *J. Phys. A* **10**, 1115 (1977).
- ³³A. Dua and B. J. Cherayil, *J. Chem. Phys.* **109**, 7011 (1998).
- ³⁴G. S. Chirikjian and Y. Wang, *Phys. Rev. E* **62**, 880 (2000).
- ³⁵G. S. Chirikjian and A. B. Kyatkin, *Engineering Applications of Noncommutative Harmonic Analysis* (CRC, Boca Raton, 2000).
- ³⁶G. S. Chirikjian and A. B. Kyatkin, *J. Fourier Analysis and Applications* **6**, 583 (2000).
- ³⁷G. S. Chirikjian, *Comput. Theor. Polym. Sci.* **11**, 143 (2001).
- ³⁸J. C. Marini, S. D. Levene, D. M. Crothers, and P. T. Englund, *Proc. Natl. Acad. Sci. U.S.A.* **79**, 7664 (1982).
- ³⁹P. C. Van der Vliet and C. P. Verrijzer, *BioEssays* **15**, 25 (1993).
- ⁴⁰J. Perez-Martin, F. Rojo, and V. De Lorenzo, *Microbiol. Rev.* **58**, 268 (1994).
- ⁴¹R. E. Dickerson, D. Goodsell, and M. L. Kopka, *J. Mol. Biol.* **256**, 108 (1996).
- ⁴²H. G. Hansma, K. A. Browne, M. Bezanilla, and T. C. Bruice, *Biochemistry* **33**, 8436 (1994).
- ⁴³J. Griffith, M. Bleyman, C. A. Rauch, P. A. Kitchin, and P. T. Englund, *Cell* **46**, 717 (1986).
- ⁴⁴R. C. Bash, J. M. Vargason, S. Cornejo, P. S. Ho, and D. Lohr, *J. Biol. Chem.* **276**, 861 (2001).
- ⁴⁵D. M. Crothers, T. E. Haran, and J. G. Nadeau, *J. Biol. Chem.* **264**, 7093 (1990).
- ⁴⁶B. Benoff, H. Yang, C. L. Lawson, G. Parkinson, J. Liu, E. Blatter, Y. W. Ebright, H. M. Berman, and R. H. Ebright, *Science* **297**, 1562 (2002).
- ⁴⁷P. J. Hagerman, *Annu. Rev. Biochem.* **59**, 755 (1990).
- ⁴⁸P. J. Hagerman, *Biochim. Biophys. Acta* **1131**, 125 (1992).
- ⁴⁹W. K. Olson and V. B. Zhurkin, in *Proceedings of the Ninth Conversation in the Discipline Biomolecular Stereodynamics*, (1996) Vol. 2, p. 341.
- ⁵⁰W. K. Olson, N. L. Marky, R. L. Jernigan, and V. B. Zhurkin, *J. Mol. Biol.* **232**, 530 (1993).
- ⁵¹C. Rivetti, C. Walker, and C. Bustamante, *J. Mol. Biol.* **280**, 41 (1998).
- ⁵²W. Miller, *Commun. Pure Appl. Math.* **17**, 527 (1964).
- ⁵³W. Miller, *Lie Theory and Special Functions* (Academic, New York, 1968).
- ⁵⁴N. J. Vilenkin, E. L. Akim, and A. A. Levin, *Dokl. Akad. Nauk SSSR* **112**, 987 (1957).
- ⁵⁵N. J. Vilenkin and A. U. Klimyk, *Representation of Lie Groups and Special Functions* (Kluwer Academic, Dordrecht, 1991).
- ⁵⁶M. E. Taylor, *Ann. Global Analysis and Geometry* **22**, 179 (2002).
- ⁵⁷A. B. Kyatkin and G. S. Chirikjian, *App. Comput. Harmonic Anal.* **9**, 220 (2000).